Polyhedral Oligomeric Silsesquioxane (POSS) Based Resists: Material Design Challenges and Lithographic Evaluation at 157 nm

Evangelia Tegou,[†] Vassilios Bellas,[†] Evangelos Gogolides,[†] Panagiotis Argitis,*,[†]
David Eon,[‡] Gilles Cartry,[‡] and Christophe Cardinaud[‡]

*Institute of Microelectronics, NCSR "Demokritos", 15310 Ag. Paraskevi, Athens, Greece, and
Laboratoire des Plasmas et des Couches Minces, Institut des Materiaux "Jean Rouxel",
BP 32229, 44322 Nantes, France*

In this paper we describe the lithographic behavior and related material properties of a new class of chemically amplified, positive tone, silicon-containing methacrylate photoresists incorporating the polyhedral oligomeric silsesquioxane (POSS) group as the etch-resistant component. POSS-bearing monomers were copolymerized with methacrylic acid (MA), *tert*-butyl methacrylate (TBMA), *tert*-butyl trifluoro methacrylate (TBTFMA), itaconic anhydride (IA), and 2-(trifluoromethyl) acrylic acid (TFMA), in various compositions. A perfluorooctylsulfonate-based photoacid generator (PAG) was used to deprotect TBMA (or TBTFMA) to base soluble carboxylic acid by heating after exposure. XPS and angular XPS analysis were used to examine possible surface segregation phenomena. It was proven that POSS surface enrichment occurs for the POSS−TBMA copolymers while surface segregation may be reduced if suitable additional resist components are selected. The POSS-based resists were studied for 157-nm lithographic applications and found to have high sensitivity (<10 mJ/cm^2 under open field exposure), no silicon outgassing, and sub-100-nm resolution capabilities. Ninety nanometer patterns in 100-nm thick films were resolved. At present, their absorbance is high (∼4 μm^{-1}) for single-layer lithographic applications at 157 nm; however, high etch resistance in oxygen plasma makes them suitable for bilayer schemes.

1. Introduction

The research activity on new lithographic resist materials capable of meeting the constantly increasing performance demands posed by the International Technology Roadmap for Semiconductors for the next decade has greatly expanded during recent years.[1] Currently, different lithographic approaches are investigated for the fabrication of devices with sub-100-nm critical dimensions, including 193 nm, 157 nm, EUV (13 nm), and e-beam based technologies and it is not yet clear which approach will dominate in each of the future technology nods.[2] In this context the research on new lithographic materials is also spread in quite a few directions and different classes of polymers are investigated as main components of the future resist systems.

In the case of 157-nm lithography, in particular, the problem of selecting polymers that can serve as the basis of the resist compositions is more severe due to the difficulty in finding organic materials with acceptable absorbance characteristics.[3−5] Partially fluorinated materials are mostly considered as the resists of choice at this wavelength, due to the high transparency of the C−F bond, although nonoptimized, so far imaging and etch resistance properties have been reported.[6−11]

On the other hand, siloxanes and silsesquioxane polymers can offer an alternative route since Si−O bonds are also quite transparent at 157 nm. In addition, these materials can also be used as thin imaging layers in bilayer schemes that would relax to some degree the transparency demands.[12−14] Although undesirable chemi-

* To whom correspondence should be addressed. Tel: +30210 6503114. Fax: +30210 6511723. E-mail: P.Argitis@imel.demokritos.gr.
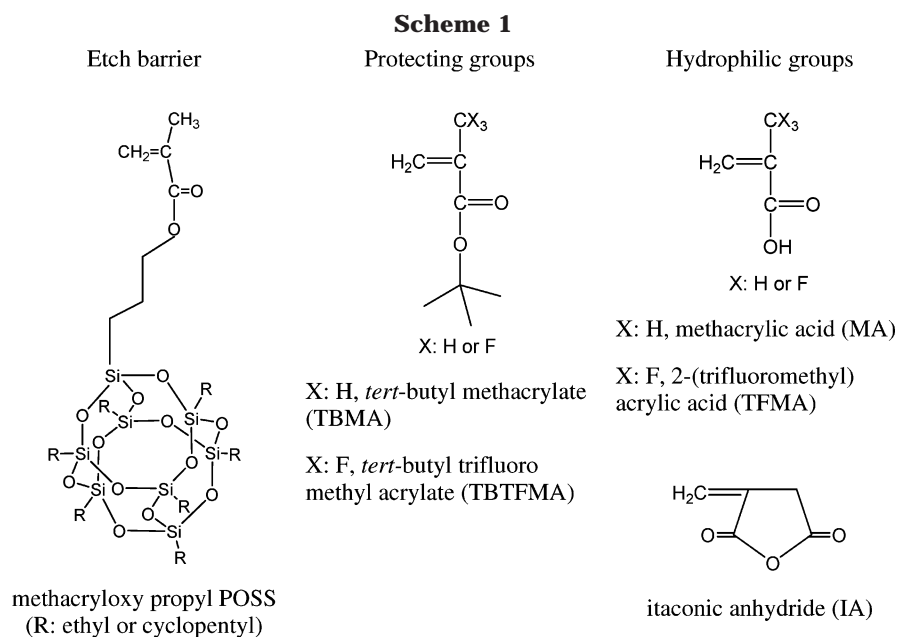† Institute of Microelectronics, NCSR "Demokritos".
‡ Institut des Materiaux "Jean Rouxel".

(1) International Technology Roadmap for Semiconductors, http://public.itrs.net.
(2) Ronse, K. *Microelectron. Eng.* **2003**, *67−68*, 300.
(3) Kunz, R. R.; Bloomstein, T. M.; Hardy, D. E.; Goodman, R. B.; Downs, D. K.; Curtin, J. E. *Proc. SPIE* **1999**, *3678*, 13.
(4) Kishimura, S.; Katsuyama, A.; Sasago, M.; Shirai, M.; Tsunooka, M. *Jpn. J. Appl. Phys.* **1999**, *38*, 7103.
(5) Yamazaki, T.; Itani, T. *Jpn. J. Appl. Phys.* **2002**, *41*, 4065.
(6) Tran, H. V.; Hung, R. J.; Chiba, T.; Yamada, S.; Mrozek, T.; Hsieh, Y.; Chambers, C. R.; Osborn, B. P.; Trinque, B. C.; Pinnow, M. J.; MacDonald, S. A.; Willson, C. G.; Sanders, D. P.; Connor, E. F.; Grubbs, R. H.; Conley, W. *Macromolecules* **2002**, *35*, 6539.
(7) Bae, Y. C.; Douki, K.; Yu, T.; Dai, J.; Schmaljohann, D.; Koerner, H.; Ober, C. K.; Conley, W. *Chem. Mater.* **2002**, *14*, 1306.
(8) Trinque, B. C.; Chiba, T.; Hung, R. J.; Chambers, C. R.; Pinnow, M. J.; Osburn, B. P.; Tran, H. V.; Wunderlich, J.; Hsieh, Y.-T, Thomas, B. H.; Shafer, G.; DesMarteau, D. D.; Conley, W.; Willson, C. G. *J. Vac. Sci. Technol. B* **2002**, *20*, 531.
(9) Toriumi, M.; Shida, N.; Yamazaki, T.; Watanabe, H.; Ishikawa, S.; Itani, T. *Microelectron. Eng.* **2002**, *61−62*, 717.
(10) Itani, T.; Toriumi, M.; Naito, T.; Ishikawa, S.; Miyoshi, S.; Yamazaki, T.; Watanabe, M. *J. Vac. Sci. Technol. B* **2001**, *19* (6), 2705.
(11) Sanders, D. P.; Connor, E. F.; Grubbs, R. H.; Hung, R. J.; Osborn, B. P.; Chiba, T.; MacDonald, S. A.; Willson, C. G.; Conley, W. *Macromolecules* **2003**, *36*, 1534.
(12) Lin, Q.; Katnani, A.; Brunner, T.; De Wan, C.; Fairchok, C.; LaTulipe, D.; Simons, J.; Petrillo, K.; Babich, K.; Seeger, D.; Angelopoulos, M.; Sooriyakumaran, R.; Wallraff, G.; Hofer, D. *Proc. SPIE* **1998**, *3333*, 278.
(13) Hatzakis, M.; Shaw, J.; Babich, E.; Paraszczak, J. *J. Vac. Sci. Technol. B* **1988**, *6*, 2224.

Scheme 1

Etch barrier

methacryloxy propyl POSS
(R: ethyl or cyclopentyl)

Protecting groups

X: H, *tert*-butyl methacrylate
(TBMA)

X: F, *tert*-butyl trifluoro
methyl acrylate (TBTFMA)

Hydrophilic groups

X: H, methacrylic acid (MA)

X: F, 2-(trifluoromethyl)
acrylic acid (TFMA)

itaconic anhydride (IA)

cal routes leading to bond breaking and formation of fragments (outgassing) that could cause problems with the components of the optical systems have been well-recognized in Si-containing polymers, recent reports show that this issue is rather addressed by using siloxanes and silsesquioxanes as opposed to polymers with Si-alkyl pendant groups.[15,16] Finally, the development of suitable siloxane or silsesquioxane resists can be of use not only for 157-nm lithography but also for 193-nm, EUV, and probably other next generation lithographic regimes.[17,18]

In the above context, our group efforts have recently been launched for examining a related class of materials that contain polyhedral silsesquioxane moieties (cages) and are provided also in the form of polymerizable acrylate monomers (Scheme 1).[19–22] Polyhedral oligomeric silsesquioxanes (POSS) represent a relatively new class of well-defined materials that consist of a silicon-based inorganic cage (Si_8O_{12}) surrounded by eight organic corner groups. POSS-containing molecules have recently received a considerable amount of interest for applications in catalysis, modeling of silica surfaces and interfaces, as precursors to silicates and as polymerizable reagents.[23–25]

Especially in the case of polymerization, POSS monomers are capable of imparting desirable properties to common classes of polymeric materials. In a typical POSS-polymer, represented by the formula $P_1R_7Si_8O_{12}$, a variety of inert substituents, R, can be attached at the seven corner positions around the cage, while the remaining position is occupied by a reactive polymerizable group, P. So far, the POSS molecules have been successfully incorporated into styryls, acrylics, liquid-crystalline polyesters, siloxanes, polyamides, etc.

The cage type possesses a precisely defined structure (monodispersed silsesquioxane components) whereas our experience with ladder silsesquioxanes is that the commercially available starting materials are unreliable because their actual molecular formulas are unknown.[26] Moreover, cage structures are free from remaining silanol bonds Si−OH that are common in commercial ladder polymers and could cause condensation reactions, resulting in limited shelf life as well as negative tone chemistry.

In the present paper we report our group work on the capabilities of using POSS monomers for 157-nm lithography. In the case of 157-nm lithography, the use of thin films has been employed in order to meet the low absorbance criterion and achieve high-resolution imaging.[3,27] Incorporating the POSS cage as a pendant group in the traditionally used methacrylate platform presents the advantage of enhanced etch resistance and the possibility of employing the bilayer scheme. Nevertheless, several requirements such as low absorbance, adhesion, controlled dissolution behavior, aqueous base development, and high-resolution imaging remain to be satisfied. The incorporation of an inert bulky hydrophobic silicon group is likely to complicate resist design even further as it impacts resist physicochemical properties. Furthermore, POSS polymers were reported to form self-assembled molecular aggregates.[28,29] Therefore, the minimization of the aforementioned potential problems

(14) Hartney, M. A.; Hess, D. W.; Soane, D. S. *J. Vac. Sci. Technol. B* **1989**, *7*, 1.

(15) Hien, S.; Angood, S.; Asworth, D.; Basset, S.; Bloomstein, T.; Dean, K.; Kunz, R. R.; Miller, D.; Patel, S.; Rich, G. *Proc. SPIE* **2001**, *4345*, 439.

(16) Lippert, T.; Dickinson, J. T. *Chem. Rev.* **2003**, *103*, 453.

(17) Sooriyakumaran, R.; Fenzel-Alexander, D.; Fender, N.; Wallraff, G. M.; Allen, R. D. *Proc. SPIE* **2001**, *4345*, 319.

(18) Hatakeyama, J.; Nakashima, M.; Kaneko, I.; Nagura, S.; Ishihara, T. *Proc. SPIE* **1998**, *3333*, 62.

(19) Wu, H.; Hu, Y.; Gonsalves, K. E.; Yakaman, M. J. *J. Vac. Sci. Technol. B* **2001**, *19*, 851.

(20) Azam, Ali M.; Gonsalves, K. E.; Golovkina, V.; Cerrina, F. *Microelectron. Eng.* **2003**, *65*, 454.

(21) Wu, H.; Gonsalves, K. E. *Adv. Mater.* **2001**, *13*, 670.

(22) Bellas, V.; Tegou, E.; Raptis, I.; Gogolides, E.; Argitis, P.; Iatrou, H.; Hadjichristidis, N.; Sarantopoulou, E.; Cefalas, A. C. *J. Vac. Sci. Technol. B* **2002**, *20*, 2902.

(23) Schwab, J. J.; Lichtenhan, J. D. *Appl. Organomet. Chem.* **1998**, *12*, 707.

(24) Li, G.; Wang, L.; Ni, H.; Pittman, C. U. *J. Inorg. Organomet. Polym.* **2002**, *11*, 123.

(25) POSS Nanotechnology Conference, CA-USA, 2002.

(26) Unno, M.; Suto, A.; Matsumoto, H. *J. Am. Chem. Soc.* **2002**, *124*, 1574.

(27) Rottstegge, J.; Herbst, W.; Hien, S.; Fuetterer, G.; Eschbaumer, C.; Hohle, C.; Schweider, J.; Sebald, M. *Proc. SPIE* **2002**, *4690*, 233.

toward the design of POSS materials suitable for lithographic applications presents a great challenge.

2. Experimental Section

2.1. Materials. POSS monomers were copolymerized with other monomers, such as methacrylic acid (MA), *tert*-butyl methacrylate (TBMA), *tert*-butyl trifluoro methyl acrylate (TBTFMA), itaconic anhydride (IA), and 2-(trifluoromethyl) acrylic acid (TFMA), in various compositions (Scheme 1). ^{1}H NMR spectra were recorded on a Bruker 200-MHz instrument with CDCl$_3$ as the solvent, at 25 °C. ^{13}C NMR analysis of polymers was performed at room temperature in CDCl$_3$ or DMF-d_7, in an inverse-gated 1H-decoupled mode on a Bruker AF 250 (62.9 MHz) spectrometer. In all cases characteristic resonances were clearly present at $\delta = 3.75$ ppm ($-CH_2CH_2$-CH$_2$-cage) and $\delta = 0.6$ ppm (methylene protons adjacent to the POSS cage). Since the polymerizations were carried to near completion (>90% yields), the ratios of the starting monomers in the copolymers are similar to the feed ratios and compositional homogeneity is expected.[30–32] Note that the electron-deficient monomers IA, TFMA, and TBTFMA do not undergo homopolymerization under conventional (AIBN-initiated) radical conditions.[33,34] They were copolymerized with electron-acceptor monomers such as TBMA, forming random copolymers.

In a typical experiment 0.01 g of AIBN and 10 g of the monomers were dissolved in 30 g of dry oxygen-free tetrahydrofuran (THF). The reaction mixture was then placed in an oil bath (70 °C) for 48 h. Each polymer was isolated after precipitation in methanol. The precipitant was dissolved in THF, and the procedure was repeated twice. Finally, the copolymers were dried under vacuum (50 °C) for 2 days. Gel-permeation chromatography (GPC) analyses were carried out on a Waters Breeze1515 series liquid chromatograph with a differential refractometer (Waters 2410) as a detector.

2.2. Physicochemical Characterization. Absorption spectra in the VUV were recorded with a J.A. Woollam VUV variable angle spectroscopic ellipsometer (VASE) VU301 and/ or a SOPRA GES5-PUV spectroscopic ellipsometers. Modulated differential scanning calorimetry (MDSC) measurements were carried out with a DSC 2920 (TA Instruments) at a heating rate of 10 °C/min. The surface hydrophobicity was estimated by the contact angle formed by a deionized water (Millipore Milli-Qplus) droplet placed on the film surface, using Digidrop DGW-EWS equipment. A Perkin-Elmer Paragon Identity Check FT-NIR spectrophotometer equipped with a deuterated diglycerine sulfate detector was used to collect FT-IR spectra with resolution of 4 cm^{-1} at 64 scans. Samples were prepared on single-polished silicon substrates. The FT-IR measurements were made in transmittance mode both for thin (150 nm) and thicker (0.5−1 μm) films. The surface chemical structure of POSS copolymers has been analyzed by X-ray photoelectron spectroscopy (XPS). The Axis Ultra analyzer from Kratos analytical was used with spectral resolution of about 0.4 eV (FWMH).

2.3. Lithographic Processing. Solutions (4−6% w/w) of all polymers were prepared with either methyl isobutyl ketone (MIBK) or propylene glycol methyl ether (PGME). The photoacid generator (PAG) used in resist formulations was triphenylsulfonium perfluorooctylsulfonate. Dissolution was monitored by an in-house-constructed DRM setup equipped with a laser emitting at a wavelength of 650 nm (angle of incidence $a \sim 5°$).[35] For low resolution near UV and deep UV exposures, a Hg−Xe lamp was used, equipped with the appropriate filters; 157-nm exposures were performed at International Sematech (Austin, TX) on an Exitech microstepper (NA = 0.6, σ = 0.3) using alternating phase-shift masks.

2.4. Oxygen Plasma Etching Studies. Thin films (typical thickness: 150 nm) of POSS copolymers were spin-cast on top of 350-nm-thick hard baked novolac. Etch resistance studies of the films were performed in an inductively coupled plasma (ICP) etcher (MET) from Alcatel (composed of a cylindrical alumina source and a diffusion chamber). The temperature of the sample was controlled at 15 °C by mechanical clamping and helium backside cooling. The etching conditions were as follows: oxygen plasma (100 sccm, 10 mTorr), source power (600 W), and bias voltage (−100 V). For comparison purposes etch resistance studies were also performed in a reactor with a similar source in Nantes. The temperature was controlled at 15 °C by using a cryostat (HUBERT unistat 385) and helium circulation. The samples were etched under 10 mTorr, 800 W, and −100 V (flow rate: 40 sccm). In both systems etching rates were monitored in situ with laser interferometry and real-time spectroscopic ellipsometry (Woolam M88 system). Surface roughness was measured before and after etching in contact mode, with a Topometrics TMX 2000 atomic force microscope (AFM). The total etching time for the surface roughness measurements was equal to the etch time for the novolac end point plus 20% overetching. The total time of etching for etch rate and selectivity measurements (novolac underlayer/resist) was as high as 900% overetching.

3. Results and Discussion

3.1. Material Properties. *3.1.1. Physical Properties of POSS Copolymers.* Our motivation is to synthesize a photoresist polymer containing polyhedral silsesquioxanes. The monomers used are shown in Scheme 1. In this section we describe the various polymers synthesized and their physical properties. Each monomer employed in the acrylate platform serves a specific reason. Methacryloxy propyl POSS is used as the etch barrier imparting the required etch resistance. TBMA or TBTFMA plays the role of the protecting group which undergoes the acid-catalyzed deprotection reaction (see section 3.2.1) while hydrophilic groups such as MA or IA provide good adhesion to the substrate and increase the aqueous base solubility (dissolution promoters). The solubility of these monomers in common organic solvents (MIBK, PGME) ensures a facile spin coating, providing regular and planar surfaces.

To study the effect of the alkyl substituents on the POSS cage, we designed a methacrylate platform with either cyclopentyl-POSS (cp-POSS) or ethyl-POSS (e-POSS) as the pendant groups. On the basis of transparency, compatibility with the polymer matrix, etch resistance, surface roughness after plasma treatment, and development issues, we chose to explore further the e-POSS platforms (see section 3.2.2 and ref 22). The absorbance coefficient values of the e- and cp-POSS containing methacrylate homopolymers at 157 nm were determined to be 3.1 and 7.6 μm^{-1}, respectively (Table 1). For the present e-POSS based copolymer compositions the absorbance is considerably high for single-layer lithographic applications; that is, the imaged copolymers

(28) Waddon, A. J.; Zheng, L.; Farris, R. J, Coughlin, E. B. *Nano Lett.* **2002**, *2*, 1149.

(29) Zheng, L.; Waddon, A. J.; Farris, R. J.; Coughlin, B. E. *Macromolecules* **2002** *35*, 2375.

(30) Mormann, W.; Ferbitz, J. *Eur. Polym, J.* **2003**, *39*, 489.

(31) Haddad, T. S.; Lichtenhan, J. D. *Macromolecules* **1996**, *29*, 7302.

(32) Ferbitz, J.; Mormann, W. *Macromol. Chem. Phys.* **2003**, *204*, 577.

(33) Aglietto, M.; Passaglia, E.; Dimirabello, L. M.; Botteghi, C.; Paganelli, S.; Matteoli, U.; Menchi, G. *Macromol. Chem. Phys.* **1995**, *196*, 2843.

(34) Ito, H.; Walraff, G. M.; Fender, N.; Brock, P. J.; Hinsberg, W. D.; Mohorowala, A.; Larson, C. E.; Truong, H. D.; Breyta, G.; Allen, R. D. *J. Vac. Sci. Technol. B* **2001**, *19*, 2678.

(35) Raptis, I.; Diakoumakos, C. D. *Microelectron. Eng.* **2002**, *61–62*, 829.

D   *Chem. Mater.*   *Tegou et al.*

Table 1. Physical Properties of Synthesized POSS-Containing Copolymers

copolymer composition (% w/w)	$a\,(\mu m^{-1})$ @157 nm	$a\,(\mu m^{-1})$ @193 nm	T_g (°C)	contact angle (deg)
20 cp-POSS/80 TBMA			114	92
100 cp-POSS	7.6	4.55	350	116
20 e-POSS/80 TBMA	4.4	0.14	114	101
40 e-POSS/60 TBMA	4.0	0.42	145	100
60 e-POSS/40 TBMA	3.5	0.99		101
30 e-POSS/40 TBMA/20 MA/10 IA (resist AC−POSS-2-69)	5.2[a]	0.67	142	96
30 e-POSS/40 TBMA/10 MA/20 IA[a] (resist AC−POSS-2-71)	5.6	0.85		91
40 e-POSS/40 TBMA/20 MA[a]	5.0	0.65	153	
30 e-POSS/50 TBMA/20 MA	4.9	0.20	147	90
30 e-POSS/60 TBMA/10 MA	4.8	0.14	123	
100 e-POSS	3.1	0.17	251	101
30 e-POSS/40 TBMA/30 TFMA[a] (resist AC−POSS-2-83)	4.0		132	94
100 TBMA	6.5		100	86

[a] These materials were loaded with 5% w/w PAG.

have absorbance values in the range $4.5-5.5\ \mu m^{-1}$. Nevertheless, the absorbance value can be decreased to $4.0\ \mu m^{-1}$ by 30% fluorination.

The glass transition temperature (T_g) of the resist formulations containing polyhedral silsesquioxanes ranges from 110 to 160 °C for the materials tested (Table 1). Increase of the polyhedral silsesquioxane component increases the T_g of the material.
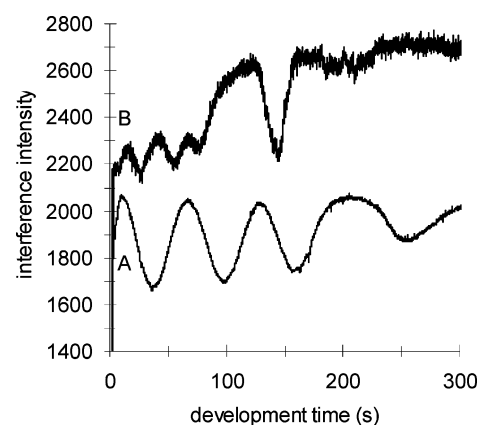
Copolymers with optimized monomer composition, namely, AC−POSS resists (ACrylate POSS, see Table 1) showed limited outgassing. The test methods applied to evaluate the outgassing probability were the film thickness loss test and the CaF_2 proof-plate test.[36] For exposure doses up to ∼30 mJ/cm², <2.5-nm loss occurred, while no silicon was detected on a CaF_2 proof-plate as was verified by XPS analysis for all AC−POSS resists.

All synthesized e-POSS copolymers are hydrophobic, independently of the POSS content. The water contact angle was measured to be in the range from 90° to 101° for POSS contents 20−100% w/w (Table 1). In addition, no significant difference in the contact angle was measured after the TBMA deprotection.

3.1.2. XPS Analysis of POSS Copolymer-Based Films.
3.1.2.1. Motivation. Some of the e-POSS ($C_{28}H_{46}O_{14}Si_8$) based copolymers have presented unusually inhomogeneous wet development. For these specific copolymers, the dissolution rate is not constant: faster dissolution takes place initially while, as film thickness decreases, slower dissolution appears. In some materials, a pronounced delay step is also present during the last period of oscillation of the DRM signal. Typical DRM signals of two POSS copolymers with optimized (signal A) and nonoptimized (signal B) development processes are shown in Figure 1. Signal B is a representative signal of POSS copolymers showing the aforementioned problems. We suspected that development problems could be due to surface segregation (similar to what has been observed for random fluorine-containing copolymers[37]) or even self-organization phenomena.[27,28] To clarify whether surface segregation was present, we used XPS analysis.[38]

3.1.2.2. XPS Results. XPS analysis gives the surface chemical composition (XPS is a surface analysis tech-

(36) Hien, S.; Angood, S.; Ashworth, D.; Basset, S.; Bloomstein, T.; Dean, K.; Kunz, R. R.; Miler, D.; Patel, S.; Rich, G. *Proc. SPIE* **2001**, *4345*, 439.
(37) Baradie, B.; Shoichet, M. S. *Macromolecules* **2003**, *36* (7), 2343.
(38) Eon, D.; Cartry, G.; Cardinaud, C., to be submitted to JVST.

Figure 1. Typical DRM signals of two POSS copolymers with optimized (signal A, AC−POSS-2-71) and nonoptimized (signal B, AC−POSS-2-69) development processes.

nique and the maximum depth probed is about 10 nm). If POSS cages reside preferentially on the surface, the surface chemical composition measured by XPS should be different from the bulk chemical composition.

Carbon (C 1s), oxygen (O 1s), and silicon (Si 2p) XPS peaks have been recorded and analyzed. The whole surface of each of the three peaks has been employed to calculate the relative surface atomic percentages (carbon, oxygen, and silicon). The carbon peak deconvolution has been used to quantify the Si−C bond percentage and the oxygen peak deconvoluion has been used to determine the Si−O bond percentage in the material. The C=O bond is well-resolved by the XPS analyzer and its measured percentage can be easily determined from the C 1s peak. If POSS groups reside preferentially on the surface, XPS analysis should indicate a higher percentage of Si−C and Si−O bond than expected from the chemical structure of the copolymer without surface segregation. Si atomic percentage should also be higher than expected. Furthermore, the C=O bond should decrease in percentage.

Table 2 presents XPS results for different copolymers. Differences between measured percentages ("meas") and expected ones ("th"), divided by expected ones, are given in percent ($100 \times [\%_{meas} - \%_{th}]/\%_{th}$). Such a representation gives the relative importance of the surface segregation phenomena for the different copolymers. If no surface segregation is present, the surface composition obtained by XPS should be equal to the bulk composition. High positive values for Si, C−Si, and O−Si together with a high negative value for C=O denote

Table 2. XPS Analysis of POSS-Containing Copolymers[a]

copolymer composition (theoretical and confirmed by NMR) POSS/TBMA/MA/IA/TFMA (% w/w)	100/0/0/0/0	60/40/0/0/0	40/60/0/0/0	20/80/0/0/0	30/50/20/0/0	30/60/10/0/0	30/40/10/20/0	30/40/0/0/30
Si (%) (from C, O, and Si peaks)	4.8 (0.9)	64.0 (6.6)	95.5 (6.3)	197.0 (6.3)	85.5 (4.1)	73.0 (3.5)	83.5 (4.0)	96.0 (4.8)
C−Si bond (%) (from C peak)	−2.5 (−0.5)	58.5 (5.9)	82.5 (8.0)	212.5 (6.8)	87.5 (4.2)	87.5 (4.2)	37.5 (1.8)	98.0 (4.9)
O−Si bond (%) (from O peak)	−7.0 (−2.0)	44.0 (6.8)	92.0 (9.0)	162.0 (7.6)	85.0 (6.2)	97.5 (7.1)	92.0 (6.6)	90.0 (6.7)
C=O bond (%) (from C peak)	−17.5 (−0.4)	−52.0 (−3.0)	−51.0 (−3.7)	−35.5 (−3.1)	−37.0 (−3.4)	−34.5 (−3.0)	−30.5 (−2.2)	−37.5 (−3.1)

[a] The Si atomic and the C−Si, O−Si, and C=O bond relative differences ($100 \times [\%_{meas} - \%_{th}]/\%_{th}$) are shown. Also in parentheses the absolute differences ($\%_{meas} - \%_{th}$) are given.
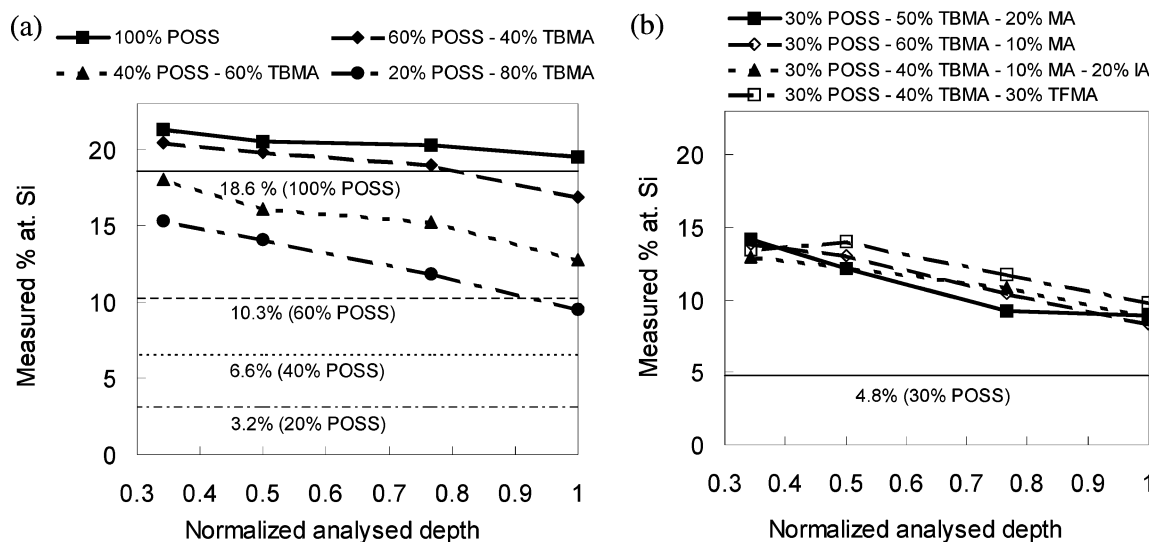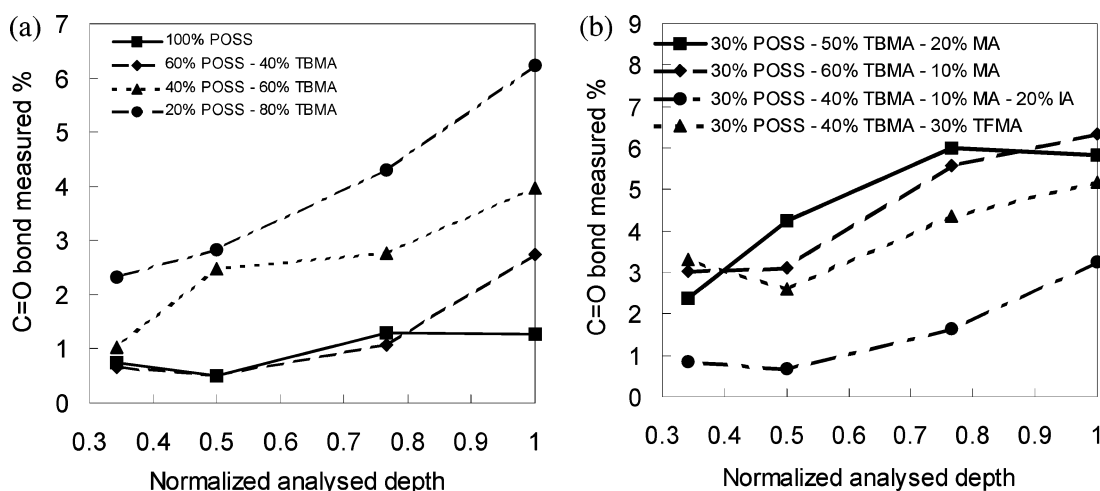

Figure 2. Angular XPS measurements: the silicon content versus the analysis angle. Also indicated on this graph by horizontal lines, theoretical percentages for materials without surface segregation.

strong surface segregation phenomena. For purposes of completeness, the values in parentheses also provide the absolute differences ($\%_{meas} - \%_{th}$).

The second column of the table presents measurements for the e-POSS homopolymer. No strong surface segregation is expected since in this case the polymer contains only POSS moieties. Therefore, all differences in the second column should be zero. Clearly, these differences do not exceed 10% (except for C=O bond percentage, 17.5%). Moreover, a positive value for the Si percentage together with negative values for C−Si and O−Si bond percentages are observed. Surface segregation should lead to positive values for Si percentage as well as for C−Si and O−Si bond percentages. Hence, results for the e-POSS homopolymer do not evidence strong surface segregation phenomena. Furthermore, the intense deviation of the C=O bond to negative values (−17.5%) is attributed to the orientation of the cage group to the film surface and the consequent encryption of the C=O bond from the free surface. On the contrary, for POSS-containing copolymers, XPS measurements point out surface segregation of POSS groups. For instance, for those consisting of 20% w/w e-POSS and 80% w/w TBMA (column 5 in Table II), the increase of the silicon content with respect to a material without surface segregation is about 200%, and that the C−Si and O−Si bond percentages exceed the

expected ones by more than 150%. The C=O bond presents a decrease of about 35%. Therefore, this material, as well as other POSS-containing copolymers, shows strong surface segregation effects. Moreover, for the members of the homologous series of POSS-TBMA copolymers, surface segregation phenomena increase with decreasing POSS percentage (columns 2−5). Incorporation of an additional hydrophilic monomer (whether MA, IA, or TFMA) seems to slightly decrease surface segregation. Actually, a 30% POSS containing material with at least three monomers (i.e., columns 6−8) presents suppressed surface segregation phenomena compared to the 40% POSS containing copolymer (column 4).

Angular XPS measurements have also been employed in order to verify further the hypothesis of surface segregation. When the analysis angle increases, the depth probed by XPS decreases. Angle equal to 0° (analyzer perpendicular to the surface) gives the maximum probed depth, D ($5 < D < 10$ nm). If the angle is equal to 60°, the probed depth is $D \cos 60° = D/2$ (40° corresponds to 0.77D probed depth and 70° to 0.34D). Thus, high analysis angles probe low sampling depths. Since XPS analysis has shown that the POSS groups reside preferentially on the surface, it is expected that, as the analysis angle decreases, that is, as we move from low probed depths ("surface" of the polymer film) to the

Figure 3. Angular XPS measurements: The C=O bond percentage versus the analysis angle.
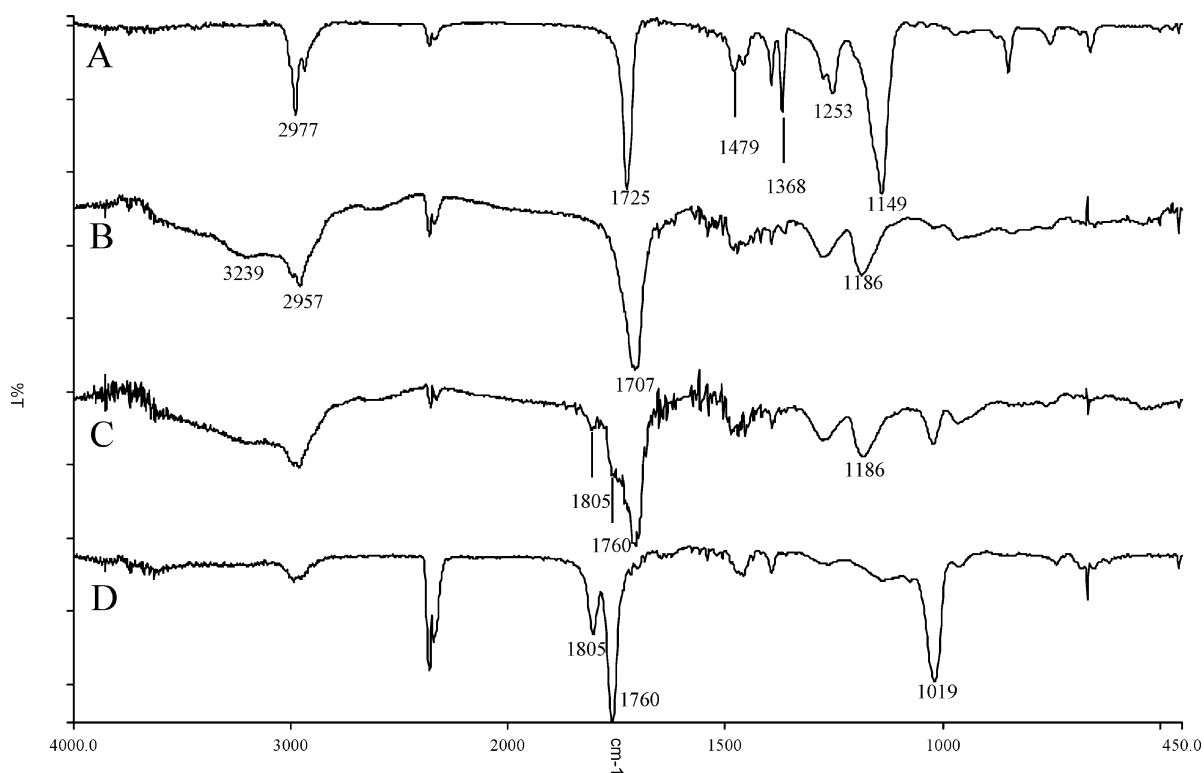
Figure 4. FT-IR spectra of PTBMA films after various processing conditions. (A) No exposure; (B) exposure dose: 203 mJ/cm², PEB: 90 °C; (C) exposure dose: 203 mJ/cm², PEB: 150 °C; (D) exposure dose: 203 mJ/cm², PEB: 225 °C.

370 maximum probed depth ("bulk"), the Si percentage
371 decreases and the C=O bond percentage increases
372 (Figures 2 and 3). For example, this is the case for the
373 copolymer comprising 20% w/w e-POSS and 80% w/w
374 TBMA, while for the POSS-based terpolymers the Si
375 content decrease and the C=O bond percentage increase
376 seem less pronounced (Figures 2b and 3b). Notice that
377 in both plots even for the e-POSS homopolymer (100%
378 POSS) there is a slight slope of the curve.

379 The values shown in Table 2 and the angular mea-
380 surements shown in Figures 2 and 3 seem to indicate
381 reduced surface segregation for terpolymers (POSS/
382 TBMA/MA or TFMA) or quarter polymers (POSS/
383 TBMA/MA/IA). A smooth development process for the
384 quarter polymers containing IA has been observed while
385 development difficulties have been encountered for
386 terpolymers containing 20% MA. The appropriate poly-

387 mer design can lead to a lithographically useful mate-
388 rial; however, at present, correlations between devel-
389 opment difficulties and surface segregation have not
390 been clearly established.

391 **3.2. Lithographic Studies.** Having studied the
392 physical properties, we proceed to examine the chemical
393 reactions during (a) imaging and (b) oxygen plasma
394 etching.

395 *3.2.1. Acid-Catalyzed Imaging in POSS Copolymers.*
396 As was proven by XPS analysis, the presence of POSS
397 groups in the studied copolymers induces surface seg-
398 regation phenomena. This could affect the course of the
399 photogenerated acid-induced deprotection reaction that
400 takes place after the PEB step. For monitoring the
401 deprotection reaction in AC−POSS copolymers, FT-IR
402 spectra were recorded. Pure PTBMA was used as a
403 reference material. Both materials were loaded with

<center>**Scheme 2**</center>
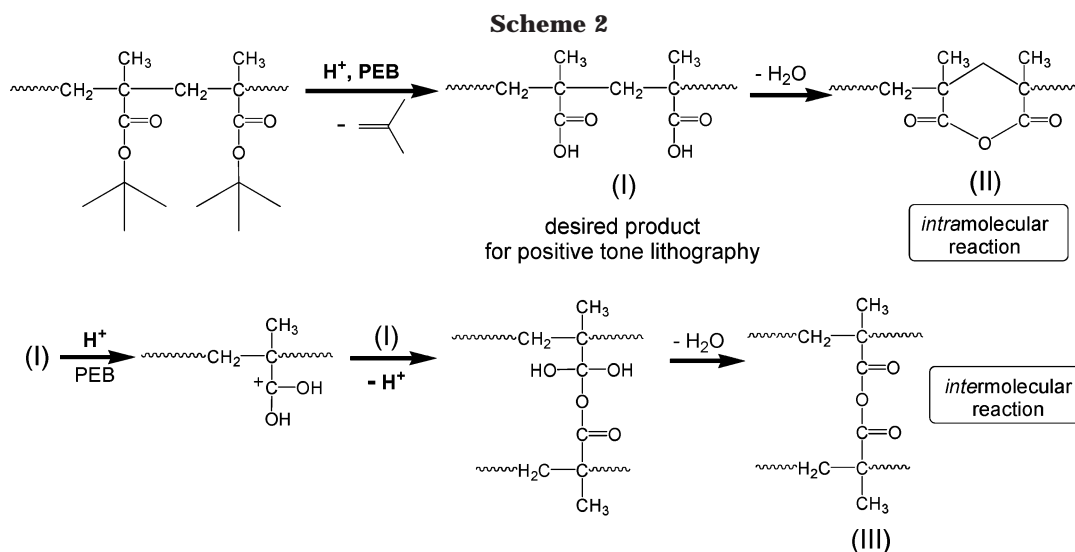
404 photo acid generators (5% w/w triphenylsulpfonium
405 perfluorooctylsulfonate for the AC−POSS copolymer
406 and 10% w/w triphenylsulfonium hexafluoroantimonate
407 for PTBMA). Processing conditions inducing similar or
408 stronger chemical effect were chosen for PTBMA to
409 ensure an accurate peak determination.

410 First, the reference material spectra are studied. In
411 Figure 4 the spectra of PTBMA for bake conditions
412 similar to the ones used for AC−POSS copolymers are
413 shown. In spectra B, C, and D extremely high exposure
414 dose (203 mJ/cm²) was used. Spectrum A corresponds
415 to a PTBMA film after the prebake step (150 °C, 2 min).
416 The peak at 1725 cm⁻¹ is assigned to the C=O bond of
417 the ester group. In spectrum B the ester group has
418 undergone the deprotection reaction, producing the
419 corresponding carboxylic acid (product I in Scheme 2).

420 Thus, the C=O peak has moved to 1707 cm⁻¹. Notice
421 also the broad peak at approximately 3200 cm⁻¹ at-
422 tributed to the O−H stretch vibration of the acid. In
423 spectrum C the PEB temperature is higher than spec-
424 trum B. As is evident in the spectrum, the deprotection
425 reaction proceeds to the formation of the carboxylic acid
426 as the main product while anhydrides (peaks at 1760
427 and 1805 cm⁻¹) start to form in an inter- or an
428 intramolecular fashion (Scheme 2). Finally, spectrum
429 D corresponding to the highest PEB temperature (225
430 °C) shows a complete disappearance of the C=O of the
431 corresponding carboxylic acid and a 100% anhydride
432 formation. Attempts to dissolve this film prove that the
433 anhydride-containing product is significantly less soluble
434 to the standard tetra methylammonium hydroxide
435 (TMAH) 0.26 N solution.
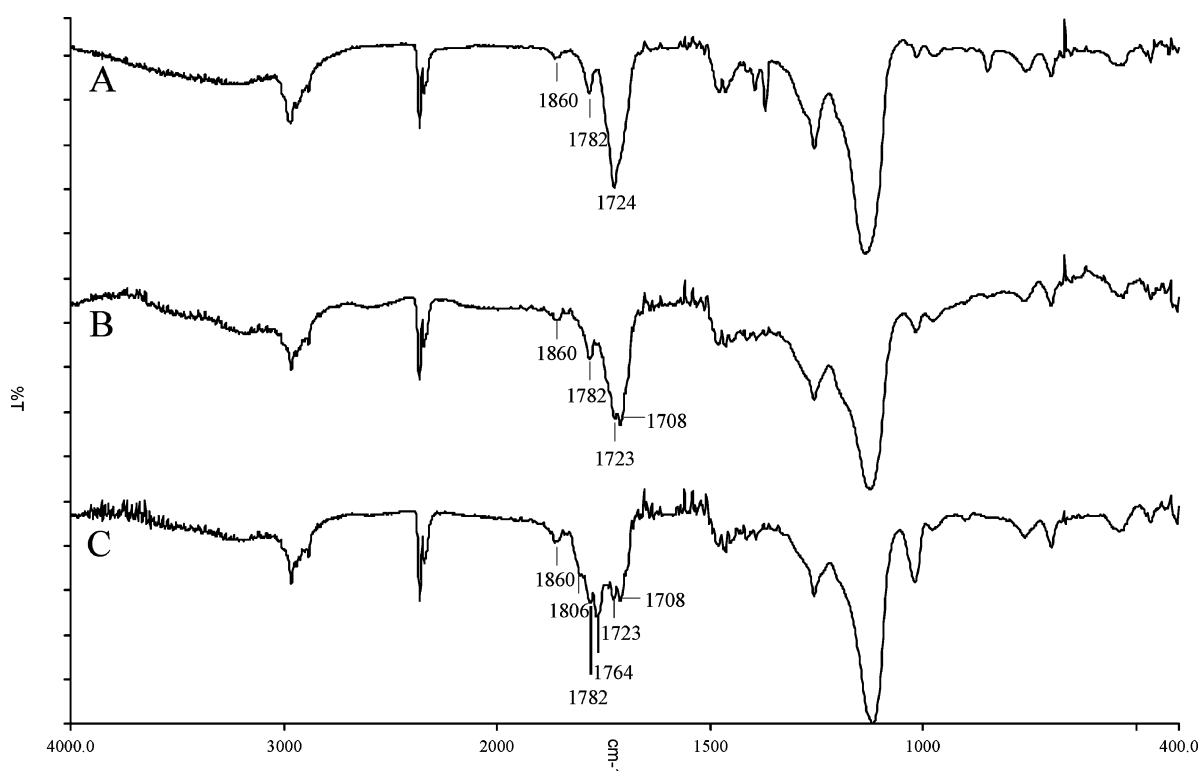
Figure 5. FT-IR spectra of AC−POSS film after various processing conditions. (A) No exposure; (B) exposure dose: 1 mJ/cm², PEB: 160 °C; (C) exposure dose: 23 mJ/cm², PEB: 160 °C.
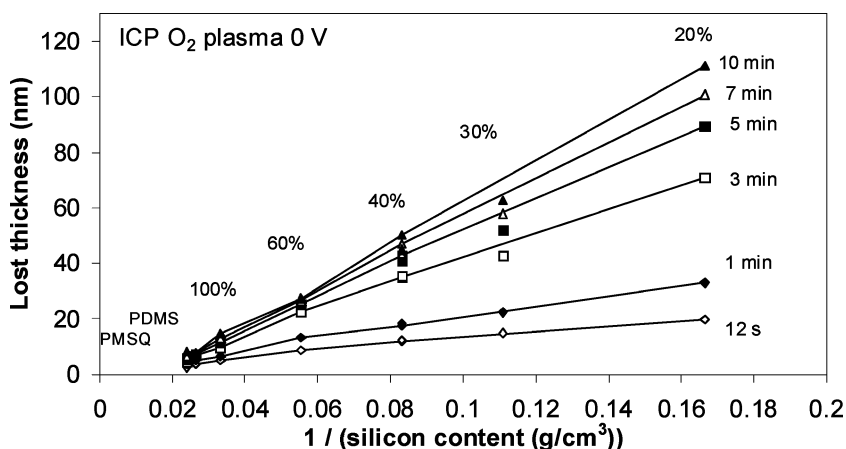
Figure 6. Thickness loss versus 1/silicon content, after various etching times in ICP oxygen plasma with 0 V bias. Comparison with poly dimethyl siloxane (PDMS) and poly methyl silsesquioxane (PMSQ).

Second, the FT-IR spectra for the AC−POSS films after various processing conditions are presented in Figure 5. The AC−POSS was comprised of e-POSS, TBMA, MA, and IA. The AC−POSS spectra, even after the prebake step (160 °C, 2 min), are more complicated than the PTBMA spectra due to the initial presence of three different types of C=O stretch vibrations. For example, in spectrum A (Figure 5) the TBMA C=O peak appears at 1724 cm^{-1} and the MA C=O appears as a broadening of the ester peak to smaller wavelengths while the IA C=O can be identified by the twin peaks at 1782 and 1860 cm^{-1}. Spectrum B shows the same material after exposure and bake. The dose was 1 mJ/cm^2, corresponding to the lithographic useful dose. The spectrum shows a decrease of the ester C=O peak at 1723 cm^{-1}, while the carboxylic acid C=O peak, produced at 1708 cm^{-1} after the *tert*-butyl ester deprotection, appears, similar to spectrum B in Figure 4 (product I in Scheme 2). For the longer exposure time (23 mJ/cm^2, spectrum C) two new bands at 1806 and 1764 cm^{-1} attributed to the formed anhydride bonds by neighboring acid functionalities appear (products II and III in Scheme 2). DRM results prove that the dissolution rate of the highly exposed AC−POSS film (spectrum C) is significantly lower than the rate of the film exposed with the lithographically useful dose (spectrum B).

FT-IR spectroscopy is an effective tool in monitoring the chemical reactions during acid-catalyzed imaging. Carboxylic acid is formed for lithographically useful doses in AC−POSS films during the ester deprotection. In a more detailed examination of spectra C in Figures 4 and 5, we notice that, in AC−POSS films, the carboxylic acid C=O peak (1708 cm^{-1}) has weakened significantly while the anhydride peaks (1764 and 1806 cm^{-1}) are well-resolved. It seems that, for similar bake temperatures, the deprotection reaction proceeds to anhydride formation in AC−POSS films to a higher extent than in the case of PTBMA films, even though for AC−POSS the exposure dose was almost 10 times lower than that for PTBMA. It is suggested that the POSS cages in the copolymer matrix favor the neighboring of the deprotected −COOH groups and, thus, the intra- or intermolecular anhydride formation at milder baking conditions. However, no negative tone behavior has been observed for doses up to 30 mJ/cm^2 (see section 3.3)

3.2.2 Etching of POSS Copolymers in an Oxygen Plasma. Cyclopentyl-substituted POSS copolymers show less etch resistance and higher surface roughness compared to ethyl-substituted copolymers. At only 20% overetching the surface roughness of the cp-POSS was ∼15 nm (rms value) while, on the contrary, e-POSS films showed only ∼0.3-nm surface roughness. This signifies that e-POSS films are appropriate for high-resolution imaging where small roughness is necessary. The reason for this difference might lie in the inherent POSS morphology: it is possible that during etching cp-POSS is stripped by the surrounding organic cyclopentyl groups and the larger distance between the cp-POSS units compared to the e-POSS units preventing the formation of a smooth oxide surface.

The etching of e-POSS copolymers containing various contents of e-POSS monomer, and hence various silicon contents, was studied with in situ spectroscopic ellipsometry and laser interferometry. A series of POSS copolymers containing 20% to 100% w/w e-POSS was etched and compared with poly methyl silsesquioxane (PMSQ) and cross-linked poly dimethyl siloxane (PDMS). Polymers containing 30% or higher w/w (i.e., 9% Si content) e-POSS cages provide the necessary etch resistance as well as low surface roughness to oxygen plasma etching at 100-nm film thickness.[22] In addition, the etch resistance of the fluorinated polymer (30% w/w e-POSS) is adequate and similar or even better to the etch resistance of the nonfluorinated polymer.[39,40]

The thickness loss is a strong function of the POSS content and decreases as the POSS content increases as shown in Figure 6. At each etching time we observe a linear relation between the lost thickness and the inverse of silicon content in the material. In addition, all polymers exhibit a very fast initial thickness loss (large etching rate), followed by a much slower etching rate. Although for PMSQ, PDMS, and 100% e-POSS the etching rate seems to stabilize to constant values, for smaller POSS contents the etching rate is higher and constantly decreases. The first fast thickness loss is attributed to etching of the organic groups from the film surface, while the subsequent etching rate reduction is

(39) Gogolides, E. International Patent Application PCT/GR03/0018/ 2003-02472.
(40) Tegou, E.; Bellas, V.; Gogolides, E.; Argitis, P.; Dean, K.; Eon, D.; Cartry, G.; Cardinaud, C. *Proc. SPIE* **2003**, *5039*, 453.
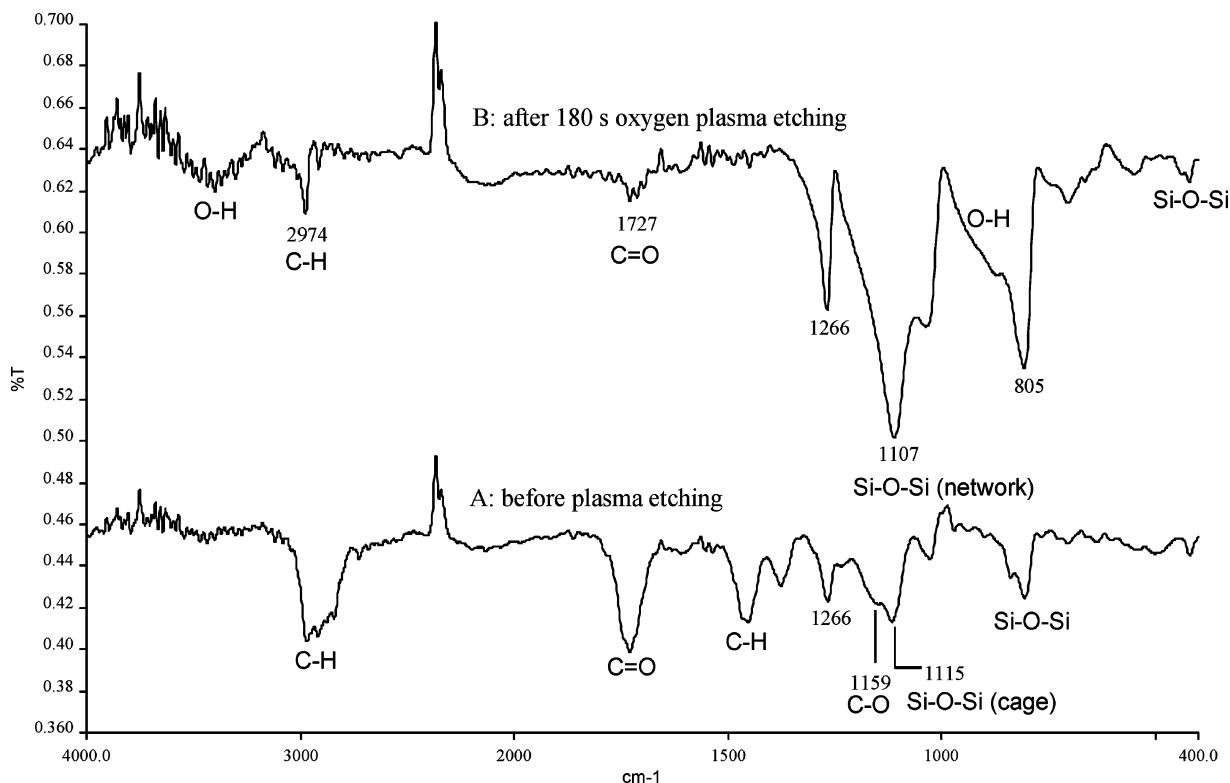
Figure 7. (A) Copolymer consisting of e-POSS, TBMA, MA, and IA before plasma etching (film thickness: 147 nm on 350-nm hard baked novolac); (B) copolymer consisting of e-POSS, TBMA, MA, and IA after 150 s of oxygen plasma etching (film thickness: 70 nm). In both spectra the novolac spectrum has been subtracted.

attributed to oxide sputtering and the densification to form an oxide. A similar mechanism has been proposed for PDMS; however, more studies are necessary to determine the surface oxide layer thickness for POSS materials.[41]

FT-IR spectroscopy has been used for detecting the formation of the SiOx layer during the oxygen plasma etching. Figure 7 shows the FT-IR spectra of a copolymer (components: POSS, TBMA, MA, IA) before etching (spectrum A) and after 150 s of etching (spectrum B). The following peaks exist in spectrum A and become significantly weak after oxygen-plasma treatment (spectrum B): 2970 cm^{-1}, attributed to C−H stretching; 1454 and 1371 cm^{-1} to C−H bending; 1734 cm^{-1} to C=O stretching; 1156 cm^{-1} to C−O stretching. On the other hand, peaks that become predominant in spectrum B are the peaks corresponding to the silicon-containing part of the copolymer, that is, at 1112 cm^{-1} corresponding to Si−O−Si asymmetrical stretch, the peak at 805 cm^{-1} assigned to Si−O−Si bending, and the peak at 450 cm^{-1} assigned to Si−O−Si wagging.[42] The slight shift (∼6 cm^{-1}) of the Si−O−Si stretching peak to lower wavelengths as well as the shoulder band around 1138−1249 cm^{-1} suggests the transformation of the cage structure to a network structure.[43] The wide bands between 3100 and 3700 cm^{-1} (O−H stretching) and 857−993 cm^{-1} (O−H out-of-plane deformation) as well as the peak at 1266 cm^{-1} (O−H bending; also Si−C

stretching) could be attributed to vibration modes of Si−OH or/and some adsorbed moisture.[44] These data point to a strong oxidation of the POSS layer and formation of an oxide-like surface. Notice that C−H, C=O, and Si−C bonds still exist to a certain extent after oxygen plasma since oxide resides only on the surface, although Si−C could be present due to residues of organic fragments. These results have also been confirmed by XPS analysis.[45]

3.3. Lithographic Evaluation. As for other acrylate-based systems, typical lithographic properties, that is, development behavior, developer strength, and imaging capabilities, depend strongly not only on the particular molecular structure of the POSS moieties but also on the copolymer composition. AC−POSS resists (see Table 1) show homogeneous development and provide materials with good film-forming properties, and high sensitivity at 157 nm (1−10 mJ/cm^2 under open field exposure). Positive tone imaging at 157 nm was obtained. Negative tone behavior has not been observed even at high doses (doses up to 10 times higher than the clearing dose have been examined). At present, due to the incorporation of MA in the copolymer formula, low-strength developers are necessary.

157-nm evaluation of the POSS copolymers was carried out at Resist Test Center at International Sematech. Phase shift masks were used for high-resolution experiments. Four AC−POSS resists were

(41) Tserepi, A.; Cordoyiannis, G.; Patsis, G. P.; Constantoudis, V.; Gogolides, E.; Valamontes, E. S.; Eon, D.; Peignon, M. C.; Cartry, G.; Cardinaud, C.; Turban, G. *J. Vac. Sci. Technol. B* **2003**, *21*, 174.
(42) Zhu, H.; Ma, Y.; Fan, Y.; Shen, J. *Thin Solid Films* **2001**, *397*, 95.
(43) Liu, W.-C.; Yang, C.-C.; Chen, W.-C.; Dai, B.-T.; Tsai, M.-S. *J. Non-Cryst. Solids* **2002**, *311*, 233.

(44) Mor, Y. S.; Chang, T. C.; Liu, P. T.; Tsai, T. M.; Chen, C. W.; Yan, S. T.; Chu C. J.; Wu, W. F.; Pan, F. M.; Lur, W.; Sze, S. M. *J. Vac. Sci. Technol. B* **2002**, *20*, 1334.
(45) Gogolides, E.; Tegou, E.; Vourdas, N.; Bellas, V.; Brani, O.; Argitis, P.; Tserepi, A.; Eon, D.; Cartry, G.; Cardinaud, C. *Proceedings 16th ISPC*, Taormina, Italy, 2003.
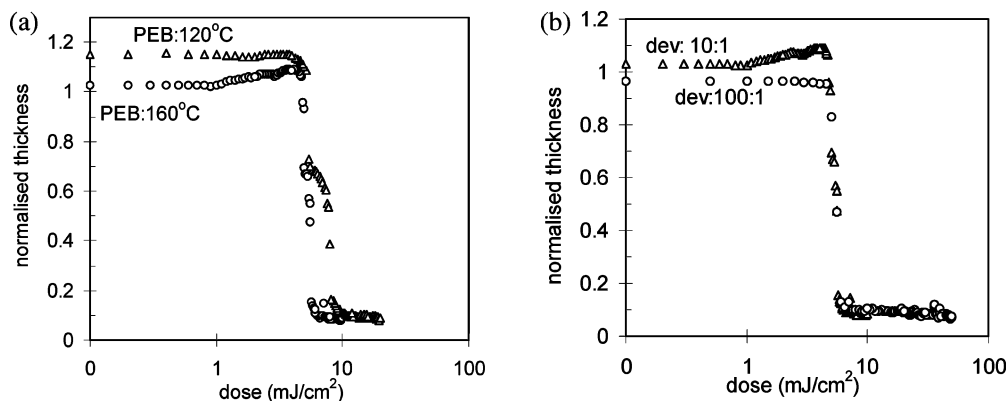
Figure 8. Contrast curves of resist AC−POSS-71. (a) Effect of PEB temperature on swelling (developer dilution 1:10, PB: 160 °C). (b) Effect of development conditions on swelling (PEB: 160 °C).
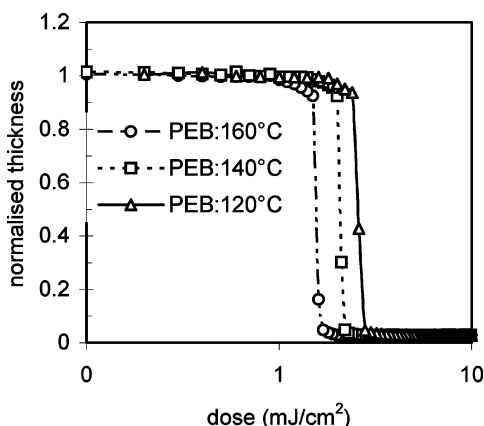
Figure 9. Contrast curves of resist AC−POSS-2-83 showing the effect of PEB temperature on resist's sensitivity (developer dilution 1:150, prebake: 120 °C).

580 evaluated, namely, AC−POSS-2-69, AC−POSS-2-71,
581 AC−POSS-2-83, and AC−POSS-2-106 (composition: 40%
582 w/w e-POSS, 40% w/w TBTFMA, and 20% w/w MA). For
583 all resist formulas PAG content was 5% w/w. The films
584 evaluated were approximately 100-nm thick. Prebake
585 and PEB temperature varied between 120 and 160 °C.
586 Diluted developer solutions (MF CD 26, Shipley) were
587 used for all resists, usually 100:1 H_2O/MF CD 26% v/v
588 or more dilute. In most experiments the development
589 conditions (developer concentration and time) were
590 nonoptimized.
591   In Figure 8a the contrast curves of the AC−POSS-2-
592 71 resist for two different PEB temperatures are

593 presented. Upon comparison of the two figures, we
594 notice the effect of PEB temperature on resist litho-
595 graphic performance. At high PEB temperatures (160
596 °C), the resist contrast is improved and the swelling is
597 reduced (notice that at 120 °C the normalized thick-
598 ness is higher than 1.0). For unexposed film areas or
599 for areas that have received very low doses, 160 °C
600 PEB temperature has the same effect as a prolonged
601 PB step (see also data in ref 40). Swelling is also affected
602 by the development conditions (Figure 8b). For strong
603 development conditions (developer dilution 1:10), swell-
604 ing takes place while, for more optimized development
605 conditions (developer dilution 1:100), no swelling is
606 observed.

607   However, for the fluorinated resist AC−POSS-2-83,
608 as shown in Figure 9, no effect of PEB temperature on
609 swelling or on contrast was observed, presumably due
610 to the inherent morphology of the sample. The improved
611 contrast as well as the high sensitivity are attributed
612 to the constructive partnership between POSS cages
613 and fluorinated components. To our knowledge, POSS
614 cage compatibility with the fluorine-containing groups
615 is demonstrated for the first time.

616   Lithographic evaluation is shown in Figure 10 for
617 AC−POSS-2-69 and AC−POSS-2-71 and in Figure 11
618 for the fluorinated resists. For high-resolution exposures
619 alternating phase shift masks were used. The results
620 show the potential of the platform, although further
621 optimization is necessary. On the other hand, first
622 pattern transfer attempts have shown the feasibility of
623 POSS-based copolymers as bilayer resists (Figure 11c).
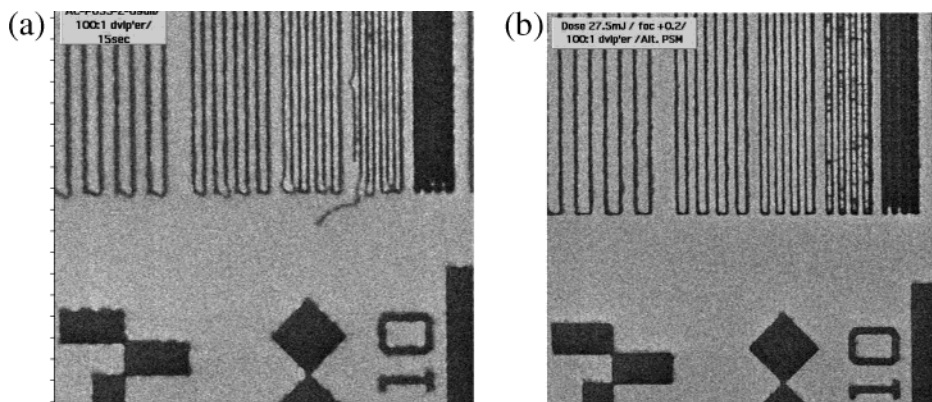
Figure 10. (a) Resist AC−POSS-2-69 showing resolution: 100 nm, l/s 1:1.5 (dose: 27.5 mJ/cm²). (b) Resist AC−POSS-2-71, resolution: 100 nm, l/s 1:2 (dose: 9.0 mJ/cm²).
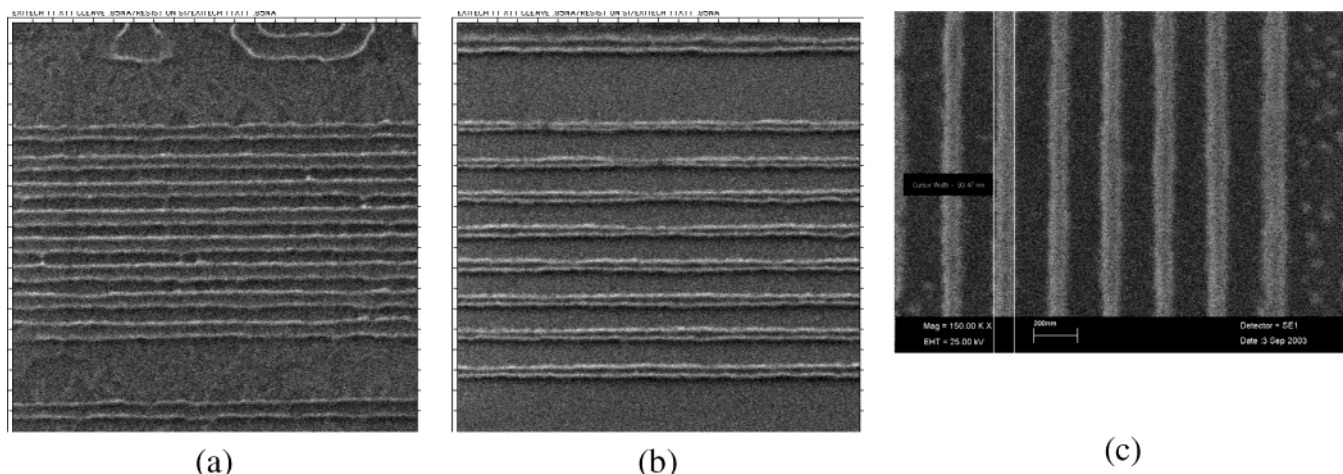
Figure 11. (a) Resist AC−POSS-2-83 showing resolution: 100 nm, l/s 1:1 (dose: 25.0 mJ/cm²). (b) Resist: AC−POSS-2-106, resolution: 100 nm, l/s 1:1.5 (dose: 24.0 mJ/cm²). (c) Resist AC−POSS-2-106 after partial dry development of the underlayer with pure O_2 plasma. Resolution: 90 nm, l/s 1:1.5 (dose: 20.5 mJ/cm²).

4. Conclusions

Copolymers bearing polyhedral oligomeric silsesquioxane (POSS) pendant groups with optimized monomer composition provide materials with good film-forming properties and high sensitivity at 157 nm (1−10 mJ/cm² under open field exposure). Selection of suitable monomers and optimized ratios are necessary for the avoidance of undesirable segregation phenomena. Process studies reveal a strong influence of thermal processing conditions and development concentrations on swelling of unexposed and underexposed resist areas. High-resolution patterning under these conditions has shown potential for sub-100-nm lithography. Partial fluorination can improve substantially absorbance properties as well as the lithography contrast at 157 nm, with no degradation of film physicochemical properties and related lithographic performance. On the other hand, pattern transfer studies have shown that 100-nm-thick films of POSS-containing materials provide the necessary oxygen plasma resistance for use as bilayer resists.

CM035089X